Research

Surface modification toughening of partially stabilized zirconia ceramics: by sub-eutectoid solution annealing

M. El-Sayed Ali[1] · S. El-Houte[1] · Omyma H. Ibrahim[1] · Kolthoum I. Othman[1] · A. A. Hassan[1]

Received: 27 March 2023 / Accepted: 22 May 2023
Published online: 09 June 2023

Abstract
In this investigation, surface modification toughening of partially stabilized zirconia ceramics, by sub-eutectoid solution annealing, has been performed. The $Zr_{0.918}Mg_{0.068}Y_{0.014}O_{1.925}$ designated (MZY) was prepared by mixing Magnesia Partially Stabilized Zirconia (MZ9) and Yttria Tetragonal Zirconia (TZ3Y) Polycrystal commercial powders using wet ball milling. The mechanical properties and microstructure of the MZY were investigated. XRD and SEM were used for phase analysis and microstructure examination of the sintered samples' surfaces. The fracture toughness and hardness of the sintered compacts were determined by the Vickers indentation technique. The physical and mechanical properties of MZY were compared to those of MZ9 ceramics prepared under the same conditions. The results showed that, the Yttria addition inhibited the exaggerated growth of the tetragonal precipitates during sintering. The MZY showed a maximum in the fracture toughness of 12.9 MPa√m upon sub-eutectoid solution annealing at 1000 °C for 150 h, while the tetragonal precipitates in the MZ9 lost coherence due to their spontaneous massive transformation to the monoclinic phase via the decomposition reaction.

Article Highlights

- Surface modification of MZY by sub-eutectoid solution annealing enhance fracture toughness.
- Yttria addition inhibited the exaggerated growth of the tetragonal precipitates during sintering.
- The MZY produced is a good ceramic material for high temperature applications due to its high thermal stability.

Keywords Sub-eutectoid · Solution annealing · Transformable tetragonal precipitates · Surface modification toughening · Decomposition reaction

1 Introduction

The surface boundary of a material is an envelope that acts as a phase barrier between the bulk and the surrounding environment, whether solid, liquid, or gas. It usually contains defects: point defects such as vacancies or interstitials, line defects like dislocations, surface flaws, cracks, and cavities [1]. A surface containing broken bonds of the material ions might attract impurities from the environment to react with or adsorb gases or liquids. So, surface modification by Surface texturing [2], or machining and polishing is a necessary step to remove the contaminants and cracks.

Zirconia toughened ceramics possess high strength and fracture toughness, giving these materials their

✉ Omyma H. Ibrahim, omyma_essam@yahoo.com | [1]Metallurgy Department, NRC Nuclear Research Centre, Egyptian Atomic Energy Authority, Cairo, Egypt.

importance as structural and bio-ceramics [3-8]. The high ionic mobility renders them useful in high-temperature fuel cells [9, 10] and oxygen sensors [11]. Due to their interesting, versatile properties, zirconia ceramics have drawn the attention of researchers for decades. Many dopants and co-dopants such as: MgO, CaO, CeO_2, Gd_2O_3, Y_2O_3, Yb_2O_3… etc., have been used to stabilize the cubic, tetragonal and meta-stable tetragonal phases in zirconia ceramics [12-17].

The doped zirconia products possess different physical, thermal, mechanical, and electrical properties; depending on the type of dopant, its concentration, processing method as well as the surface treatment. An important aspect in this concern, is the properties/microstructure dependence [18-21] and the ability of the material to retain the tetragonal phase symmetry upon cooling to room temperature after sintering [3, 6, 22].

Among the doped zirconia ceramics, magnesia partially stabilized zirconia Mg-(PSZ) could be obtained with a magnificent microstructure, giving extraordinary properties to this material. In the seventies, Garvie [23] discovered the great aspect of transformation toughening in zirconia ceramics, which led him to call this material "ceramic steel". He showed that the stress which associated transformation of the metastable tetragonal precipitates to the monoclinic phase changed this brittle ceramic material into a tough one. Partially stabilized zirconia is widely used as an advanced technical ceramic material because of its enhanced fracture toughness and nonlinear stress–strain behaviour. The outstanding mechanical properties of Mg-(PSZ) result from solid state phase transformation at regions of high stress concentration which creates a great resistance to crack evolution. This stress-induced transformation requires the existence of a considerable amount of the transformable tetragonal phase, a goal which can be achieved through changing various parameters such as: microstructure, grain size and chemical composition [22].

In order to improve the mechanical properties of partially stabilized zirconia ceramics, surface treatment or modification could have a beneficial effect. The surface of the sintered Mg-(PSZ) material could be modified by a wide variety of methods, to induce phase transformation on the sample surface, which increases strength and fracture toughness [22, 24, 25].

The surface modification in this respect serves to generate compression stress in the sample surface layer. It can be performed through mechanical, chemical [26], or thermal means. The first mechanism (the mechanical surface treatment) includes grinding, polishing and sand-blasting [27]. It is based on the stress driven phase transformation of the metastable tetragonal phase to the monoclinic phase. In the latter two methods, the destabilization of the surface layer through dopant depletion results in transformation of the coherent metastable tetragonal phase precipitates to a monoclinic phase plus free magnesia. Increasing the transformable tetragonal precipitates on the surface of these PSZ ceramic materials, through coarsening the fine non-transformable tetragonal precipitates during solution annealing, might be an interesting way of surface modification that leads to the enhancement of the fracture toughness [28].

Despite having good mechanical properties, this interesting ceramic material shows a lack of long-term phase and structure stabilities at elevated temperatures [29], which needs to be a subject of extensive research and development.

In the present work, we studied the effect of sub-eutectoid solution annealing of Mg-PSZ ceramics doped with yttria ($Zr_{0.918}Mg_{0.068}Y_{0.014}O_{1.925}$), designated as MZY. The powder was prepared by wet ball milling of commercial (9 mol%) Magnesia doped Zirconia and (3 mol%) yttria doped zirconia. The sintered compacts made from these powders were polished and sub-eutectoid solution annealed at 1000 °C for different periods of time and were subjected to the necessary examinations for microstructure and phase analysis. The surface modification of the sub-eutectoid solution annealed and its effects on the fracture toughness and the hardness of the sintered compacts have been investigated. The physical and mechanical properties of MZY were evaluated and compared to those of MZ9 ceramics prepared under the same conditions.

2 Experimental work

2.1 Materials

a. Commercial powder of magnesia partially stabilized zirconia MZ9, from TOSHO-JAPAN. The chemical analysis is given in Table 1.
b. Yttria tetragonal zirconia polycrystals TZ3YA from TOSHO-JAPAN. The chemical analysis is given in Table 2.

Table 1 MZ9 chemical analysis

Chemical analysis	Wt.%
MgO	3.23
SiO_2	0.016
Fe_2O_3	0.016
Na_2O	0.002
Al_2O_3	0.11
Ig. loss	0.9

Those powders were used to prepare $Zr_{0.918}Mg_{0.068}Y_{0.014}O_{1.925}$ (MZY).

2.2 Methods

The MZY powder was prepared by mixing 76 mol% of MZ9 and 24 mol% TZ3YA. The mixed powder was wet ball milled in ethyl alcohol using zirconia balls for 8 h. Rectangular compacts were prepared from the dried powder by pressing in a steel die (8×30 mm^2) at a pressure of 100 MPa, followed by sintering in air at 1700 °C for 4 h.

The sintered densities were determined by the water displacement "Archimedes" method. The polished sintered samples were sub-eutectoid solution annealed at 1000 °C for different periods of time. The microstructure examination was performed using both a scanning electron microscope JEOL-Japan and an optical microscope Olympus-Japan.

X-ray diffraction machine (XRD-3A) from Schimadzu-Japan has been used for phase analysis. The analyses were made on the surfaces of polished sintered as well as the solution annealed samples. The monoclinic fraction (X_m) and the volume fraction (V_m) of the monoclinic phase were calculated from the integrated peak area of $I_{t+c}(111)$ for the cubic plus tetragonal phases and I_m (111) and I_m ($\bar{1}11$) for the monoclinic phase. The following equations were used to perform these calculations [30].

$$X_m = \frac{I_m\left(\bar{1}11\right) + I_m(111)}{I_m\left(\bar{1}11\right) + I_m(111) + I_{t+c}(111)} \quad (1)$$

$$V_m = \frac{\mathcal{P}X_m}{1 + (\mathcal{P} - 1)X_m} \quad (2)$$

where $\mathcal{P}$ is a constant equal to 1.333.

Zwick hardness tester from Germany has been used for measuring the Vickers hardness HV and the fracture toughness stress intensity factor K_{IC}. The tests were performed using 200 N load for 10 s. Vickers hardness was calculated using the following equation:

$$HV = 1.854\, P/d^2 \quad (3)$$

Fracture toughness was calculated using the halfpenny-crack equation [31]:

$$K_{IC} = 0.0725\, P\, c^{-3/2} \quad (4)$$

where **P** is the indentation load in Newton (N), **d** and **c** are the mean indentation diagonal and the half crack lengths in meters, respectively. The average of 6 indentations was taken for each.

Table 2 TZ3YA chemical analysis

Chemical analysis	Wt.%
Y_2O_3	5.08
SiO_2	0.011
Fe_2O_3	0.006
Na_2O	0.007
Al_2O_3	0.10
Ig. loss	3.5

3 Results and discussion

Table 3 summarizes the physical and mechanical properties of the as-sintered MZ9 and MZY ceramics. The sintered compacts of both materials had high densities (99% of theoretical density). It can be seen from the table that the co-doping with yttria increased the Vickers hardness while the fracture toughness decreased, in agreement with previously published works [32-34].

XRD patterns are shown in Fig. 1 for MZ9 and Fig. 2 for MZY, both sintered at 1700 °C/4 h. The phase analysis showed only cubic plus tetragonal phases for MZY in contrast to MZ9 which contained in addition, 14% monoclinic phase. This amount of the monoclinic phase indicates the presence of large transformable tetragonal precipitates; that transform to the monoclinic phase upon

Table 3 Physical and mechanical properties of the as-sintered MZ9 and MZY ceramics

Material	Density % of TD	HV, GPa	K_{1C} MPa√m
MZ9	98.8 ± 0.8	9.9 ± 0.3	6.7 ± 0.26
MZY	99.7 ± 0.2	10.8 ± 0.4	5.5 ± 0.2

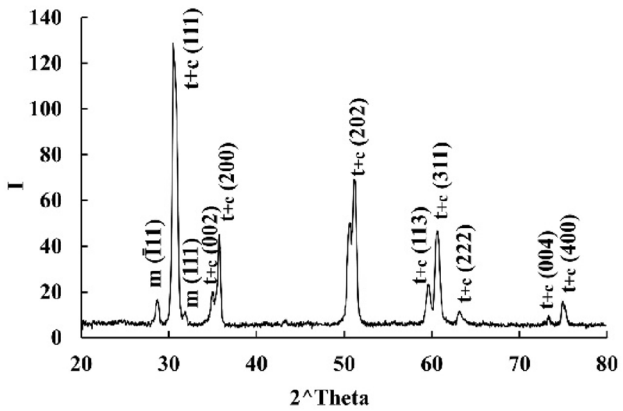

Fig. 1 XRD pattern for MZ9, sintered at 1700 °C/4 h

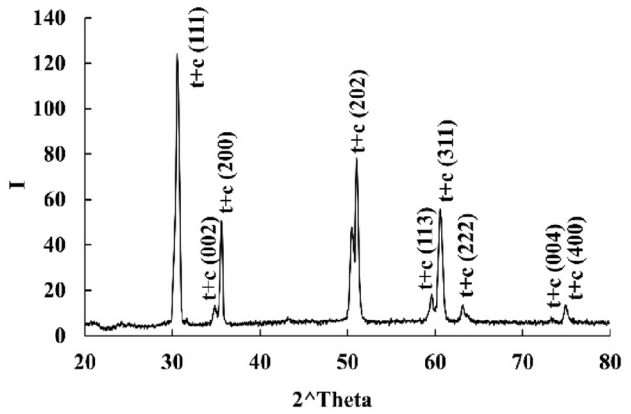

Fig. 2 XRD pattern for MZY, sintered at 1700 °C/4 h

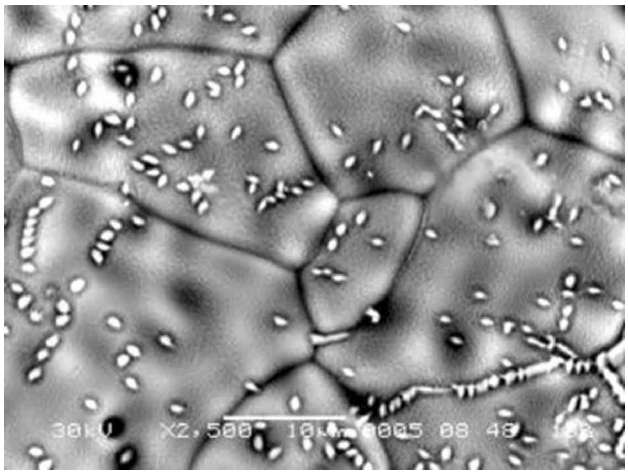

Fig. 3 SEM micrograph of the as-sintered MZ9

cooling from the sintering temperature. Recently published results showed a monoclinic content of about 50% on the sintered, 1500 °C/2 h, sample surfaces for materials prepared from dry milled powder mix of TZ3Y and Mg-PSZ (8 mol% MgO) [34]. The high monoclinic content might be attributed to the use of 8 mol% MgO in Mg-PSZ instead of 9 mol% MgO in the Mg-PSZ or due to their employing dry milling that might have produced heterogeneous powder. In contrast, Mg-PSZ and Mg-PSZ with 1.7 mol% Y_2O_3 addition, made by co-precipitation method [33], showed a comparable phase analysis to that obtained in the present work. This is explained by the heterogeneities appearing in the dry milled powder in [34] compared to the homogeneity on the molecular level scale obtained by the co-precipitation technique in [33].

Figure 3 shows the SEM micrograph of the as-sintered MZ9. It can be seen from the figure that the microstructure is composed of a cubic matrix of large grains 25 µm in size, containing very small and finely dispersed lenticular tetragonal (t) precipitates beside relatively larger oblate shape monoclinic (m) precipitates and white spots of MgO rich phase at/or near the grain boundaries. Coarsening of some tetragonal (t) precipitates during the sintering process can drive their transformation to the monoclinic phase during cooling [35, 36]. On the other hand, the SEM micrograph of the as-sintered MZY sample (Fig. 4) consists of a matrix of large cubic grains of average grain size of 40 µm containing small finely dispersed lenticular tetragonal (t) precipitates, which retained their tetragonal symmetry upon cooling from the sintering temperature. Few white spots of the magnesia-rich phase appeared in the microstructure. That is to say, the yttria addition inhibited the exaggerated growth of the tetragonal precipitates during sintering, in agreement with Yamagata et al. [32].

Figure 5 shows the zirconia rich part of the ZrO_2-MgO binary phase diagram [37]. At 1700 °C, the sintering temperature used in this investigation, the dominant phases are the cubic and the tetragonal solid solutions; while in the sub-eutectoid temperature range 1400–1240 °C, a tetragonal solid solution phase plus Magnesium Oxide prevails. At lower temperatures, below 1240 °C, the equilibrium phases are the monoclinic ZrO_2 and MgO.

In the present work, upon sub-eutectoid solution annealing at 1000 °C (in the middle of the hatched area, in which the composition of the sample used lies), a decomposition reaction of tetragonal phase (t) to the monoclinic phase (m) plus MgO might have taken place for the relatively large sized transformable tetragonal precipitates.

Figure 6 shows the fraction of the monoclinic phase formed on the samples' surfaces of both MZ9 and MZY upon annealing at 1000 °C for various periods of time. It can be seen that upon solution annealing MZ9 a substantial increase in the monoclinic phase in the sample surface occurred, which increased with annealing time. More than

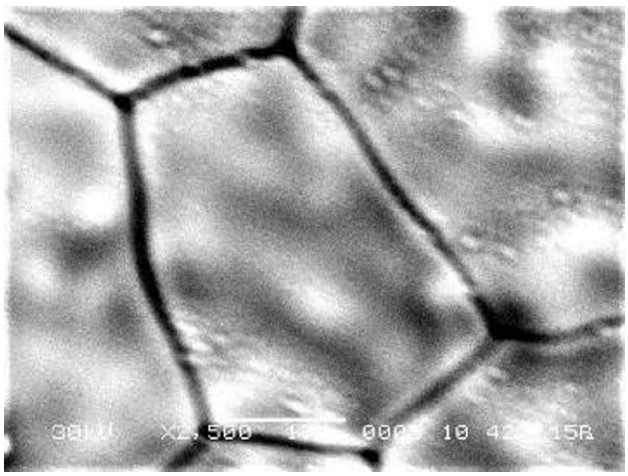

Fig. 4 SEM micrograph of the as-sintered MZY

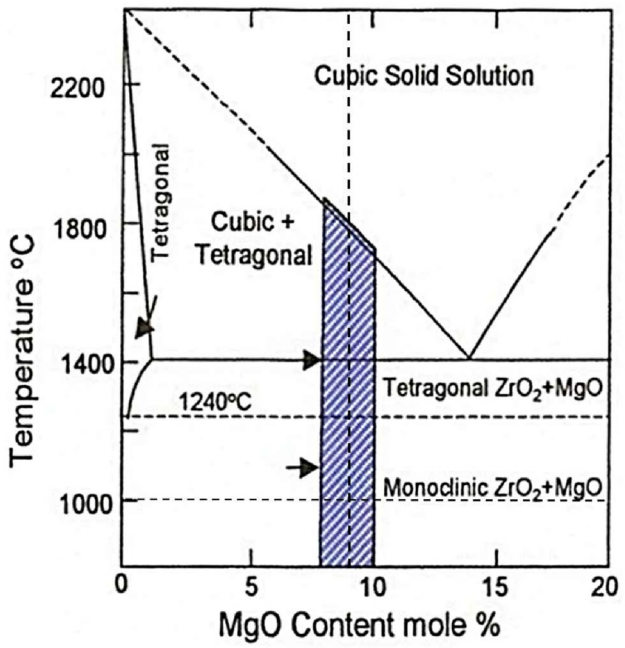

Fig. 5 The zirconia rich part of the ZrO_2–MgO binary phase diagram [37]

90% t → m transformation was measured after annealing for 240 h. This result agrees with published results [36] obtained for zirconia containing 3.6 wt.% MgO when annealed at 1000 °C. The coarsening of the transformable tetragonal precipitates causes them to lose coherency and to transform to the monoclinic (m) phase. The SEM micrograph, Fig. 7, illustrates the dramatic deterioration caused by the massive t → m transformation after 240 h sub-eutectoid solution annealing of MZ9 at 1000 °C. It shows large incoherent monoclinic precipitates, micro-cracks, black spots of large pores, and large white spots of magnesia and magnesia-rich phases.

On the other hand, the MZY samples showed resistance toward the transformation to the monoclinic phase. Only 6% of the transformable tetragonal phase was transformed to the monoclinic phase after the same annealing time. This shows clearly that the destabilization reaction proceeds at a much higher rate with the increase in the solution annealing time for MZ9 than it does in MZY, where only 23% monoclinic phase was detected on its surface after 700 h solution annealing.

Figure 8 shows the variation of the Vickers hardness HV with the annealing time. The MZ9 samples showed a dramatic decrease in the hardness, compared to the MZY samples which showed only a slight decrease. Figure 9 shows the increase in the fracture toughness of the MZY samples which reached a maximum value of 12.9 MPa√m after annealing for 150 h. Meanwhile, the toughness of MZ9 decreased from 6.7 to 3.7 MPa√m after the same annealing time. Similar behaviours have been reported after high-temperature annealing [34], and after low-temperature hydrothermal treatments as well [38-40]. The drastic effects exhibited by the MZ9 samples during sub-eutectoid solution annealing at 1000 °C/240 h are due to the massive decomposition reactions taking place.

Figure 10a shows large cracks emerging from the impression corners made by Vickers hardness indenter at indentation load 100 N, on the MZ9 sample surface annealed at 1000 °C for 240 h, compared to that made on the as sintered polished surface (Fig. 10b). Figure 11 shows the impression made on the surface of the MZY sample annealed for 720 h at 1000 °C, using the same indentation load (100 N). The micrograph shows a typical transgranular

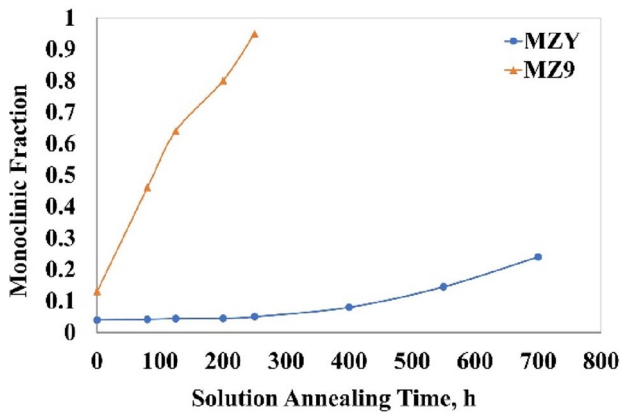

Fig. 6 The fraction of the monoclinic phase formed on the samples' surfaces of MZ9 and MZY upon annealing at 1000 °C for various periods of time

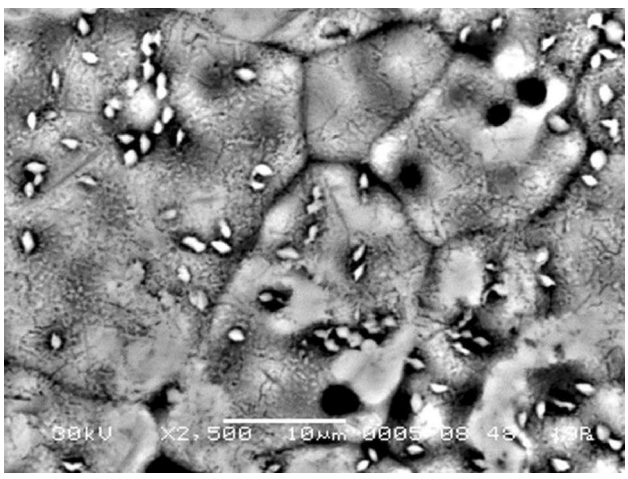

Fig. 7 SEM micrograph of MZ9 after 240 h sub-eutectoid solution annealing at 1000 °C

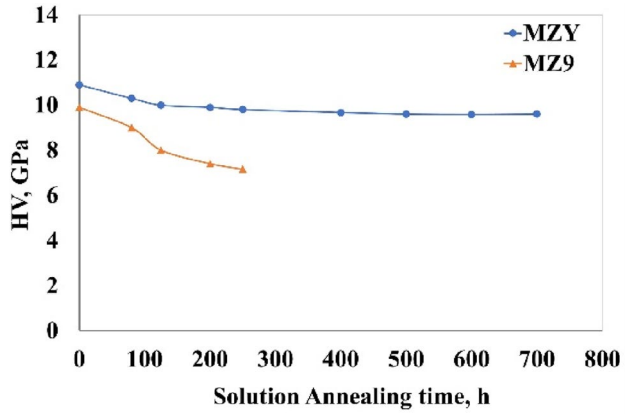

Fig. 8 The variation of the Vickers hardness HV with the annealing time for sintered MZ9 and MZY

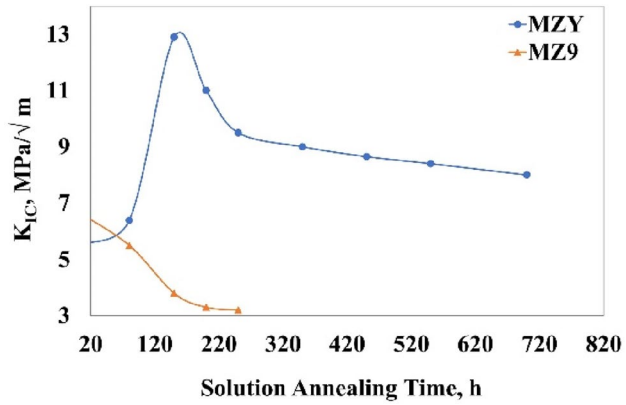

Fig. 9 The variation of the fracture toughness with the annealing time for sintered MZ9 and MZY

surface fracture; characteristic of cubic ZrO_2, in accordance with previously published results [24].

The interpretation of these results can be elucidated as follows: first, in the case of MZ9 some of the large transformable tetragonal precipitates in the cubic grains transform into a monoclinic phase upon cooling from the sintering temperature. The rapid growth rate of the metastable transformable tetragonal precipitates during sub–eutectoid solution annealing at 1000 °C, triggers their spontaneous massive transformation to the monoclinic phase via the decomposition reaction mentioned above, which leads to decohesion and loss of coherence. This results in a very weak material composed mainly of a monoclinic phase and of poor mechanical strength, as can be deduced from Figs. 6, 7, 8 and 9.

Second, the presence of yttria in addition to magnesia in MZY, produced a ceramic of large cubic grains containing fine non-transformable tetragonal precipitates as mentioned earlier. Upon sub-eutectoid solution annealing at 1000 °C, the formation of transformable tetragonal precipitates by coarsening of the fine non-transformable ones took place. More detailed, the fine precipitates gradually coarsened which led to their transformation -in escalating amounts- to the size of the transformable tetragonal precipitates, reaching its maximum after 150 h annealing time. This might explain the increase in the fracture toughness of the MZY remarked in Fig. 9; where the stress-induced transformation toughening came into action. The transformable tetragonal precipitates continue to grow with annealing time to a certain size where spontaneous transformation to the monoclinic phase occurs. This is governed by the destabilization reaction of transformable

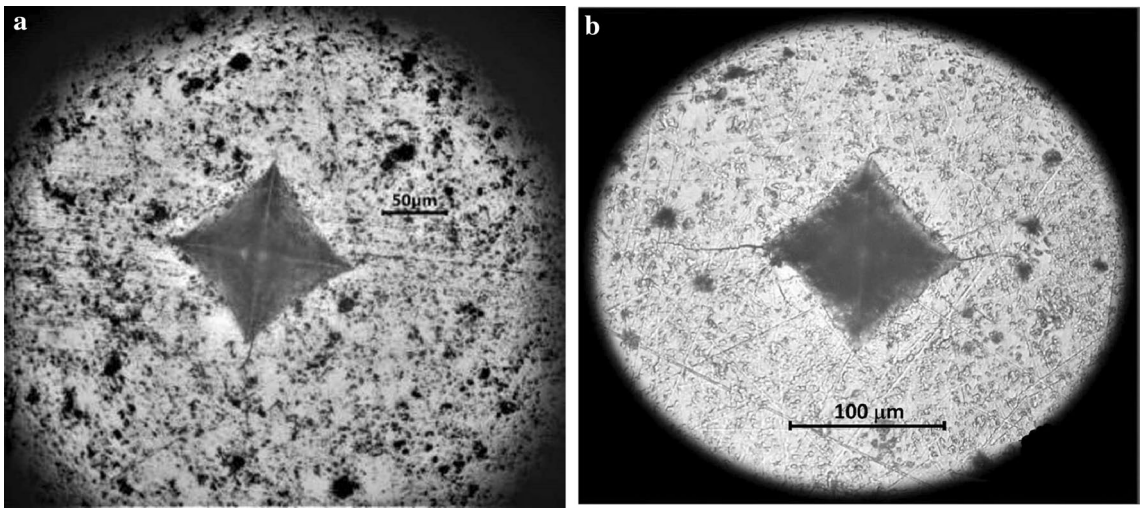

Fig. 10 **a** Optical micrograph showing impression of 100 N indentation made on the MZ9 annealed (after sintering and polishing) at 1000 °C/240 h. **b** Optical micrograph showing impression of 100 N indentation made on the polished surface of MZ9 sintered at 1700 °C/4 h

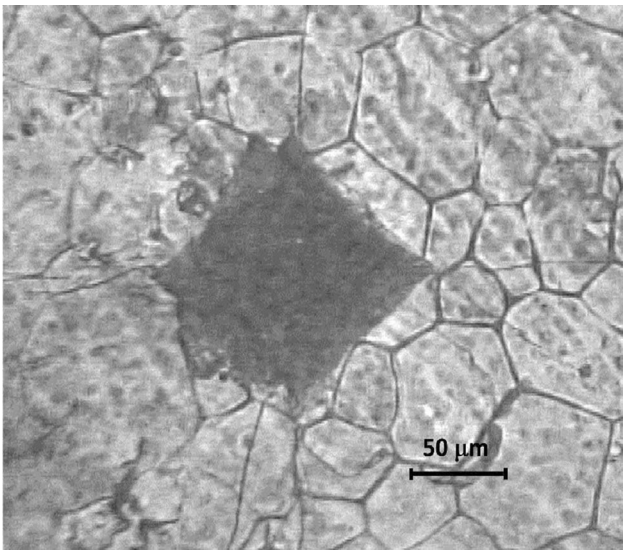

Fig. 11 Optical micrograph showing impression of 100 N indentation made on the MZY after annealing at 1000 °C/720 h

tetragonal (t) coarse precipitates to monoclinic (m) precipitates + MgO; which took place slowly due to the presence of yttria. Thus, the content of the stress-assisted transformable tetragonal precipitates decreases and consequently the fracture toughness. That is to say that during the subeutectoid annealing in the period from 0 to 150 h, the rate of formation of the stress-induced transformable tetragonal precipitates was higher than that resulting from the destabilization reaction reached after this annealing time. However, it should be noted here that the amount of the monoclinic phase resulting from the destabilization reaction was initially small and below the detection limit of the X-Ray diffractometer. Then it began to increase after 240 h annealing time. At this stage and beyond, the formation of the stress-assisted transformable tetragonal by coarsening of the remaining fine precipitates as well as the destabilization reaction of the coarse precipitates act simultaneously. The net result will be a slow rate decrease in fracture toughness. This decrease in K_{IC} of MYZ proceeded to reach a value of about 8 MPa√m after 700 h solution annealing time, which is still higher than the value measured on the as-sintered sample. The build-up of the monoclinic phase contributes to toughening by creating surface compressive stresses; due to the dilatant nature of the tetragonal to monoclinic phase transformation [22, 23, 41]. Surface compression acts against crack initiation and cracks propagation during loading, thus strengthening and toughening the material. The compressive stress decreases with the increase in the thickness of the monoclinic layer [42], following the increase in annealing time. This clearly explains the observed decrease in K_{IC} after reaching its maximum value. In general, and more specifically in zirconia ceramics, the (t) to (m) phase transformation induces compressive surface stresses [25, 43]. This is similar to the compressive surface stresses created upon the monoclinic phase formation on sample surfaces, induced by grinding [22] or even by hydrothermal annealing at relatively low temperatures which were accompanied by an increase in the flexural strength as well [38-40]. The key factor is the stress-assisted transformable tetragonal precipitates: their rate of growth and spontaneous destabilization, which is controlled by the presence of yttria. In general co-doping of zirconia ceramics results in a product of enhanced properties and better phase stability [44]. Cao et al. found that the addition of Yb_2O_3 to 8.5YSZ also showed better stability at very high temperature (1400 °C) [2].

4 Conclusion

The $Zr_{0.918}Mg_{0.068}Y_{0.014}O_{1.925}$, (MZY) powder was prepared using a wet ball milling process. The sintered compacts made from this powder were polished and sub-eutectoid solution annealed at 1000 °C for different periods of time. The findings of this research can be summarized as follows:

- The sintered compacts made from the prepared powder were dense and tough ceramics, and the phase analysis showed only cubic plus tetragonal phases for MZY.
- The yttria (in TZ3Y) addition to MZ9 inhibited the exaggerated growth of the tetragonal precipitates during sintering.
- Coarsening converts the non-transformable tetragonal precipitates to transformable ones, during solution annealing at 1000 °C, reaching a maximum after 150 h annealing time.
- K_{IC} value of 12.9 MPa√m was obtained for MZY after 150 h annealing time.
- The presence of yttria in addition to magnesia slowed down the growth rate of the tetragonal precipitates and consequently the decomposition transformation reaction of the metastable tetragonal phase to the monoclinic one upon solution annealing.
- The high thermal stability and maintenance of the high values of fracture toughness at high temperatures renders MZY a good ceramic material for high-temperature applications.

Author contributions M.Elsayed: main idea and supervisionS.Elhoute: results analysis and reviewingOmyma H. Ibrahim: did mechanical testing: hardness and fracture toughness.Kolthoum I. Othman: wrote the manuscript and made an X-ray analysisA.A. Hassan: Doing scanning electron microscopy photographs

Funding Open access funding provided by The Science, Technology & Innovation Funding Authority (STDF) in cooperation with The Egyptian Knowledge Bank (EKB). The authors have not disclosed any funding.

Declarations

Competing interests The authors declare no competing interests.

References

1. Jaeger H, Sanders JV (1968) Surface structure of defects in crystals. J Res Inst Catal Hokkaido Univ 16(1):287–303
2. Cao Z, An S, Song X (2022) Effect of thermal treatment at high temperature on phase stability and transformation of Yb_2O_3 and Y_2O_3 Co-doped ZrO_2 ceramics. Sci Rep 12(1):9955–9962
3. Tosiriwatanapong T, Singhatanadgit W (2018) Zirconia-based biomaterials for hard tissue reconstruction. Bone Tissue Regen Insights 9:1–9
4. Sengupta P, Bhattacharjee A, Maiti HS (2019) Zirconia: a unique multifunctional ceramic material. Trans Indian Inst Met 72(8):1981–1998
5. Sagir VM, Babu BP, Chirayath KJ, Mathias J, Babu R (2011) Zirconia in restorative dentistry: a review. Int J Clin Dent Sci 2(3):1–5
6. Vagkopoulou T, Koutayas SO, Koidis P, Strub JR (2009) Zirconia in dentistry: Part 1. Discovering the nature of an upcoming bioceramic. Eur J Esthet Dent 4(2):130–151
7. Gautam C, Joyner J, Gautam A, Rao J, Vajtai R (2016) Zirconia based dental ceramics: structure, mechanical properties, biocompatibility and applications. Dalton Trans 45(48):19194–19215
8. Piconi C, Maccauro G, Muratori F, Brach del Prever E (2003) Alumina and zirconia ceramics in joint replacements. J Appl Biomater Biomech 1(1):19–32
9. Singhal SC, Iwahara H (1993) Proceedings of the third international symposium on solid oxide fuel cells
10. Baumard J, Abelard P (1983) Defect structure and transport properties of ZrO2-based solid electrolytes. In: Internationalconference on the science and technology of zirconia, pp 555–571. https://inis.iaea.org
11. Okada H, Tamura T, Ramakrishnan N, Atluri S, Epstein J (1992) Analysis of toughening of magnesia partially stabilized zirconia, due to dilatational transformation. Acta Metall Mater 40(6):1421–1432
12. Aktas B, Tekeli S, Salman S (2014) Synthesis and properties of La_2O_3-doped 8 mol% yttria-stabilized cubic zirconia. J Mater Eng Perform 23:294–301
13. Thakare V (2012) Progress in synthesis and applications of zirconia. Int J Eng Res Dev 5(1):25–28
14. Aktas B (2016) Influence of borosilicate addition on mechanical properties and sinterability of 8YSZ. Acta Phys Pol A 129(4):677–679
15. Motoc AM, Valsan S, Slobozeanu AE et al (2020) Design, fabrication, and characterization of new materials based on zirconia doped with mixed rare earth oxides: review and first experimental results. Metals 10(6):746
16. Golieskardi M, Satgunam M, Ragurajan D (2014) Densification behaviour and mechanical properties of aluminium oxide and cerium oxide-doped yttria tetragonal zirconia polycrystal ceramics using two-step sintering. J Nanosci 2014:1–6
17. Llanos G (2018) Additive manufacturing of zirconia. In: Master's thesis in materials engineering Chalmars University Guthenburg Sweden
18. Jang JH, Lee J (2000) Microstructure and mechanical properties of fine-grained magnesia-partially-stabilized zirconia containing titanium carbide particles. J Am Ceram Soc 83(7):1813–1815
19. Aktas B, Tekeli S, Salman S (2016) Improvements in microstructural and mechanical properties of ZrO_2 ceramics after addition of BaO. J Ceram Int 42(3):3849–3854
20. Moradkhani A, Baharvandi H (2018) Effects of additive amount, testing method, fabrication process and sintering temperature on the mechanical properties of Al_2O_3/3Y–TZP composites. J Eng Fract Mech 191:446–460
21. Aktas B, Tekeli S (2015) Effect of Co_3O_4 on the fracture toughness and microstructure of yttria-stabilized cubic zirconia (8YSZ). Acta Phys Pol 127(4):1384–1387
22. Van den Berg P (1992) Zirconia ceramics and mechanical surface interactions. Technische Universiteit Eindhoven, Eindhoven
23. Garvie RC (1983) Structural applications of ZrO_2-bearing materials. In: Science and technology of zirconia II, pp 465–479. American Ceramic Society, Inc, Columbus, OH (USA); 2. international conference on the science and technology of zirconia; Stuttgart (Germany, F.R.), 21–23 June. https://inis.iaea.org
24. Ali MES, Houte S, E, Sørensen O, (1991) Strengthening of magnesia partially stabilized zirconia by surface modification. Ceram Int 17(5):309–314
25. Leide AJ, Todd RI, Armstrong D (2021) Effect of ion irradiation on nanoindentation fracture and deformation in silicon carbide. JOM 73(6):1617–1628
26. Takita Y, Yamakami T, Yamaguchi T, Taruta S (2021) Chemical strengthening of zirconia/swelling mica composites by ion-exchange in molten salts. J Asian Ceram Soc 9(2):598–608
27. Jakovac M, Klaser T, Radatović B et al (2021) Impact of sandblasting on morphology, structure and conductivity of zirconia dental ceramics material. Materials 14(11):2834
28. HanninkR H, Kelly PM, Muddle B (2000) Transformation toughening in zirconia-containing ceramics. J Am Ceram Soc 83(3):461–487
29. Reckziegel A (2015) Properties and applications of high-performance ceramics made of zirconia. Technical report: Aliaxis Utilities and Industry
30. Toraya H, Yoshimura M, Sōmiya SH (1984) Quantitative analysis of monoclinic-stabilized cubic ZrO_2 systems by X-ray diffraction. J Am Ceram Soc 67(9):C-183–C–184
31. Ćorić D, Ćurković L, Majić Renjo M (2017) Statistical analysis of Vickers indentation fracture toughness of Y-TZP ceramics. Trans Famena 41(2):1–16

32. Yamagata C, Mello-Castanho SRH, Paschoal JOA (2014) 21º CBECIMAT, Synthesis and Mechanical Properties of Stabilized Zirconia Ceramics: MgO–ZrO_2 and Y_2O_3–MgO–ZrO_2. Congresso Brasileiro de Engenharia e Ciência dos Materiais 09 a 13 de Novembro de 2014, Cuiabá, MT, Brasil
33. Yamagata C, Paschoal J (2011) Influence of Y_2O_3 addition on the microstructure and mechanical properties of Mg–PSZ ceramics. J Mater Sci Eng A 1:556–561
34. Soylemez B, Sener E, Yurdakul A, Yurdakul H (2020) Fracture toughness enhancement of yttria-stabilized tetragonal zirconia polycrystalline ceramics through magnesia-partially stabilized zirconia addition. J Sci Adv Mater Devices 5(4):527–534
35. Montross C (1993) Relationships of tetragonal precipitate statistics with bulk properties in magnesia-partially stabilized zirconia. J Eur Ceram Soc 11(5):471–480
36. Westmacott K, Thorel A, Broussaud D, Laval JY (1987) Microstructural changes in (Mg) PSZ during aging at 1000°C. Ultramicroscopy 22(1–4):15–26
37. Swab JJ (2001) Role of oxide additives in stabilizing zirconia for coating applications. Army Research LabAberdeen Proving Ground Md, Defense Technical Information Center, pp 1–42
38. Kontonasaki E, Giasimakopoulos P, Rigos A (2020) Strength and aging resistance of monolithic zirconia: an update to current knowledge. Jpn Den Sci Rev 56(1):1–23
39. Elsheemy AA, Bakry SI, Azer AS, Abdelrazik TM (2017) The effect of two aging methods on the flexural strength and crystal structure of yttria stabilised zirconia polycrystals (in vitro study). Alex Dent J 42(2):193–197
40. Amat NF, Muchtar A, Amril MS, Ghazali MJ, Yahaya N (2019) Effect of sintering temperature on the aging resistance and mechanical properties of monolithic zirconia. J Mater Res Technol 8(1):1092–1101
41. Heussner KH, Claussen N (1989) Strengthening of ceria-doped tetragonal zirconia polycrystals by reduction-induced phase transformation. J Am Ceram Soc 72(6):1044–1046
42. Merac MR, Bram M, Malzbender J et al (2018) Increasing fracture toughness and transmittance of transparent ceramics using functional low-thermal expansion coatings. Sci Rep 8(1):1–9
43. Rickhey F, Marimuthu KP, Lee H (2017) Investigation on indentation cracking-based approaches for residual stress evaluation. Materials 10(4):404
44. Ibrahim OH, Othman KI, Hassan AA, El-Houte S, Ali MES (2020) Effect of Gadolinia addition on the mechanical and physical properties of zirconia/ceria ceramics. SN Appl Sci 2(10):1755–1763